#141 Dupl

NUB-74-171-E

E 141
PRL

ANL/HEP 7369

Semi-Inclusive Two-Particle Rapidity Correlations in 205 GeV/c pp Interactions

R. SINGER, Y. CHO, T. FIELDS, L. G. HYMAN, and P. A. SCHREINER
Argonne National Laboratory*, Argonne, Illinois 60439

and

L. VOYVODIC, R. WALKER, and J. WHITMORE
National Accelerator Laboratory+, Batavia, Illinois 60510

and

R. ENGELMANN, T. KAFKA, and M. PRATAP
State University of New York‡, Stony Brook, New York 11790

Experimental results on two-particle correlations are given as a function of prong number for charged-charged, --, ++, and +- particles in 205 GeV/c inelastic pp collisions. Clear evidence is seen for strong positive correlations in the central region for four- and six-prong events. Selection of four-prong events with a large rapidity gap shows that the strong correlation is largely associated with diffractive-type events.

*Work supported by the U. S. Atomic Energy Commission.

+Operated by Universities Research Association Inc. under contract with the U. S. Atomic Energy Commission.

‡Work supported in part by the National Science Foundation.

In the preceding Letter,[1] inclusive two-particle rapidity correlations in 205 GeV/c pp interactions were presented and compared to a simple physical model. However, since the model uses the experimental multiplicity and semi-inclusive rapidity distributions as input, some correlation effects are implicitly included. To better isolate dynamical correlation effects and to further explore the mechanisms responsible for the observed rapidity correlations, we have studied these correlations for a fixed number of prongs (i. e. semi-inclusive correlations).

The data were obtained from an exposure of the 30-inch hydrogen bubble chamber at the National Accelerator Laboratory (NAL) to a 205 GeV/c proton beam. For the four-prong sample,[2] 1191 events have been measured in three views using the POLLY III system at Argonne National Laboratory (remeasurements were performed manually at a magnification of ~ 6 times life size). Independently, 250 four-prong events have been measured in two views using the bubble pattern matching techniques described elsewhere.[3] The individual event results obtained from the two methods agree very well. In addition, higher multiplicity events have been independently measured using the bubble pattern method at both Argonne and Stony Brook, and again the results agree.

Using the n-prong events, with cross section σ_n,[4] we have measured the two usual forms of the correlation function:

$$R^n(y_1, y_2) = [\sigma_n \frac{d^2\sigma_n}{dy_1 dy_2} / \frac{d\sigma_n}{dy_1} \frac{d\sigma_n}{dy_2}] - 1$$

$$C^n(y_1, y_2) = [\frac{1}{\sigma_n^2} \frac{d\sigma_n}{dy_1} \frac{d\sigma_n}{dy_2}] R^n(y_1, y_2)$$

with y the CM longitudinal rapidity. Note that the integrals of C^n_{cc}, C^n_{--}, C^n_{++} and C^n_{+-}, over the entire y_1, y_2 plane, are $-n$, $-n_-$, $-n_+$, and 0, respectively, and that the integral of $C^n(y_1, y_2)$ over a region Ω in rapidity space is a measure of event to event fluctuations of the number of particles (n_Ω) in Ω:

$$\int_\Omega C^n(y_1, y_2)\, dy_1 dy_2 = \langle n_\Omega (n_\Omega - 1)\rangle - \langle n_\Omega \rangle^2 .$$

In Table I are listed values of the correlation functions R^n and C^n at $y_1 \approx y_2 \approx 0$ for all topologies and all charge combinations. Due to space limitations, only results on R^n_{cc}, R^n_{--}, and R^n_{+-} for four-, six-, eight- and twelve-prong events are shown in the figures (results for cases not shown are similar). Table II lists values of the semi-inclusive single particle densities, $\rho^n = \frac{1}{\sigma_n} \frac{d\sigma_n}{dy}$, so that one can convert from R to C. Fig. 1 shows the values of $R^n_{cc}(y_1, y_2)$ versus $\Delta y = y_2 - y_1$ for $-0.25 < y_1 < 0.25$ and $-1.25 < y_1 < -0.75$. Fig. 2 shows similar plots for R^n_{--}, while Fig. 3 gives R^n_{+-}. The curves represent Monte Carlo results based on the simple model described in the previous Letter.[1] Note that for a fixed prong number, this model does not include dynamical two-particle correlations.

The following conclusions can be reached despite the modest statistical accuracy of the data:

(1) R^n_{cc}: The values of $R^n_{cc}(0, 0)$ range from -0. 11 to +0. 12 and are all within two standard deviations of zero.[5] For low multiplicities, the data lie well above the model curves for Δy near zero and below the curves for large Δy. These differences become smaller as the prong number increases. There is no major difference in the structure of R^n_{cc} when y_1 is near -1, i. e. near the end of the rapidity plateau, as compared to the case when $y_1 = 0$. This is consistent with invariance under rapidity translations.

Our values for $R^n_{cc}(0, 0)$ are consistently below the preliminary results of the Pisa-Stony Brook[6] experiment at the CERN Intersecting Storage Rings (ISR). Their data at $\sqrt{s} = 23.6$ GeV (our experiment is at $\sqrt{s} = 19.7$ GeV) show all $R^n_{cc}(0, 0)$ to be positive, e. g., $R^{4,5}_{cc}(0, 0) \approx 0.40 \pm 0.08$, $R^{6,7}_{cc}(0, 0) \approx 0.20 \pm 0.03$, with an approach toward zero as the multiplicity increases. In order to understand possible systematic differences[7] in the two experiments, we have recalculated our experimental values of $R^n_{cc}(0, 0)$, combining neighboring multiplicities together, using η_{CM}, and applying analogous acceptance criteria. We find that our results for $R^n_{cc}(0, 0)$ then become quite consistent with the ISR values.

(2) $C^n_{cc}(0, 0)$ is probably decreasing as a function of prong number. Due to the increase with n of the single particle density[3] near $y = 0$, this trend follows from the observed behavior of $R^n_{cc}(0, 0)$.

(3) R^n_{--}: Little or no additional correlation effect is observed in R^n_{--} as

compared to the model curves.

(4) R^{n}_{+-}: Here the correlations in the four-prong events are large in the central region and again fall below the model curves as Δy increases. Also, the values of R^{4}_{+-} exhibit translational invariance. R^{6}_{+-} exhibits the same properties as R^{4}_{+-}, although with a smaller central maximum. For higher multiplicities, the R^{n}_{+-} correlation effects become smaller and more consistent with the model curves.

To further investigate the large correlation effect in the four-prong events, we have selected diffractive events, defined as those having a large rapidity gap (LRG) between either the first and second or third and fourth particles (when the particles are ordered in rapidity).[2] In Fig. 3(a), the triangles correspond to those events that have this gap size larger than 2. 5 units. The events that do not have a large gap give values of R^{4}_{+-}, not shown, consistent with zero (typical errors are ± 0.1). We see from Fig. 3(a) that it is the large gap events that are giving the large value of R^{4}_{+-}. A similar selection has been made for the six-prong events and yields results similar to those found for the four-prongs, although not as pronounced. We have made the same LRG $>$ 2. 5 selection in the model and have found that the dotted curve for R^{4}_{+-} is not changed from that shown. Thus it seems that the diffractive-type events, which lie outside the scope of this simple model, are giving the large correlation in the central region for the four-prong events.

In summary, we find strong positive correlation effects in the central rapidity region, with R(0, 0) smaller for higher prong number events. These correlations are consistent with translational invariance. Moreover, the strongest central correlations seem to arise in diffractive-type four-prong events.

We thank M. Derrick, B. Musgrave, and H. Yuta for supplying data on the complete sample of four-prong events, and P. Grannis, C. Quigg, and C. N. Yang for helpful discussions.

References

1. Preceding Phys. Rev. Letters.

2. M. Derrick et al., "Diffraction Dissociation in Four-Prong Proton-Proton Interactions at 205 GeV/c," ANL/HEP 7356, to be published.

3. Y. Cho et al., Phys. Rev. Letters 31, 413 (1973).

4. G. Charlton et al., Phys. Rev. Letters 29, 515 (1972).

5. From Fig. 1(b) an estimate of $R^{6}_{cc}(0, 0) \sim 0.05 \pm 0.06$ can be made using CM symmetry and smoothness criteria, so that the tabulated value for $R^{6}_{cc}(0, 0)$ may include a large statistical fluctuation. These criteria could also be used to obtain better precision on other tabulated values.

6. G. Bellettini, "Results from the Pisa-Stony Brook ISR Experiment,"

paper given at the Fifth International Conference on High Energy Collisions, Stony Brook (1973).

7. Three possible systematic effects can contribute to the difference: (a) the presence of delta rays, e^+e^- pairs from gamma conversions, and secondary hadron showers in the ISR experiment, (b) the absence of secondaries due to a 10% loss of solid angle in the ISR experiment, and (c) the use of $\eta_{CM} = -\ln\tan[\theta_{CM}/2]$ in the ISR experiment rather than y.

Table I

Measured Values for $R^n(0, 0)$ and $C^n(0, 0)$[a]

n	$R^n_{cc}(0, 0)$	$R^n_{--}(0, 0)$	$R^n_{++}(0, 0)$	$R^n_{+-}(0, 0)$	$C^n_{cc}(0, 0)$	$C^n_{--}(0, 0)$	$C^n_{++}(0, 0)$	$C^n_{+-}(0, 0)$
4	0.12 ± 0.10	-----------	-0.29 ± 0.08	0.52 ± 0.13	0.03 ± 0.03	-----------	-0.03 ± 0.01	0.03 ± 0.01
6[b]	-0.11 ± 0.06	-0.50 ± 0.05	-0.35 ± 0.05	0.20 ± 0.07	-0.15 ± 0.08	-0.13 ± 0.01	-0.14 ± 0.02	0.06 ± 0.02
8	0.03 ± 0.04	-0.27 ± 0.05	-0.30 ± 0.04	0.06 ± 0.05	0.07 ± 0.14	-0.18 ± 0.03	-0.25 ± 0.03	0.04 ± 0.04
10	-0.04 ± 0.04	-0.06 ± 0.05	-0.22 ± 0.03	0.06 ± 0.04	-0.22 ± 0.21	-0.05 ± 0.04	-0.39 ± 0.05	0.08 ± 0.05
12	-0.05 ± 0.04	-0.19 ± 0.04	-0.20 ± 0.03	0.05 ± 0.04	-0.51 ± 0.40	-0.41 ± 0.08	-0.63 ± 0.09	0.13 ± 0.10
14	-0.11 ± 0.05	-0.07 ± 0.05	-0.19 ± 0.04	-0.08 ± 0.05	-1.23 ± 0.59	-0.19 ± 0.15	-0.68 ± 0.15	-0.25 ± 0.15

[a]For cc we use the interval $-0.25 < y < 0.25$. For the other charge combinations, the interval is $-0.5 < y < 0.5$. Note that these differ from intervals used in Refs. 2-6.

[b]See Ref. 5.

Table II

Semi-Inclusive Single Particle Densities

y	ρ_c^4	ρ_c^6	ρ_c^8	ρ_c^{12}	ρ_-^4	ρ_-^6	ρ_-^8	ρ_-^{12}	ρ_+^4	ρ_+^6	ρ_+^8	ρ_+^{12}
0.0	0.52	1.17	1.71	3.29	0.20	0.50	0.78	1.49	0.29	0.63	0.91	1.74
-0.5	0.46	1.07	1.70	3.00								
-1.0	0.50	1.05	1.47	2.85	0.18	0.42	0.63	1.16	0.32	0.61	0.91	1.53
-1.5	0.53	0.90	1.38	2.06								
-2.0	0.64	0.85	1.05	1.20	0.16	0.25	0.40	0.51	0.47	0.62	0.75	0.79
-2.5	0.76	1.01	1.05	0.85								
-3.0	0.69	0.40	0.35	0.29	0.05	0.07	0.08	0.08	0.55	0.43	0.39	0.30

Figure Captions

Fig. 1 $R^{n}_{cc}(y_1, y_2)$ versus $\Delta y = y_2 - y_1$ for fixed y_1: (a) n = 4, (b) n = 6, (c) n = 8, (d) n = 12. The curves are results of the model described in Ref. 1.

Fig. 2 $R^{n}_{--}(y_1, y_2)$ versus $\Delta y = y_2 - y_1$ for fixed y_1: (a) n = 6, (b) n = 8, (c) n = 12. The curves are results of the model described in Ref. 1.

Fig. 3 $R^{n}_{+-}(y_1, y_2)$ versus $\Delta y = y_2 - y_1$ for fixed y_1: (a) n = 4, (b) n = 6, (c) n = 8, (d) n = 12. (a) also shows the results of the large rapidity gap selection (LRG > 2.5) described in the text. The curves are results of the model described in Ref. 1.

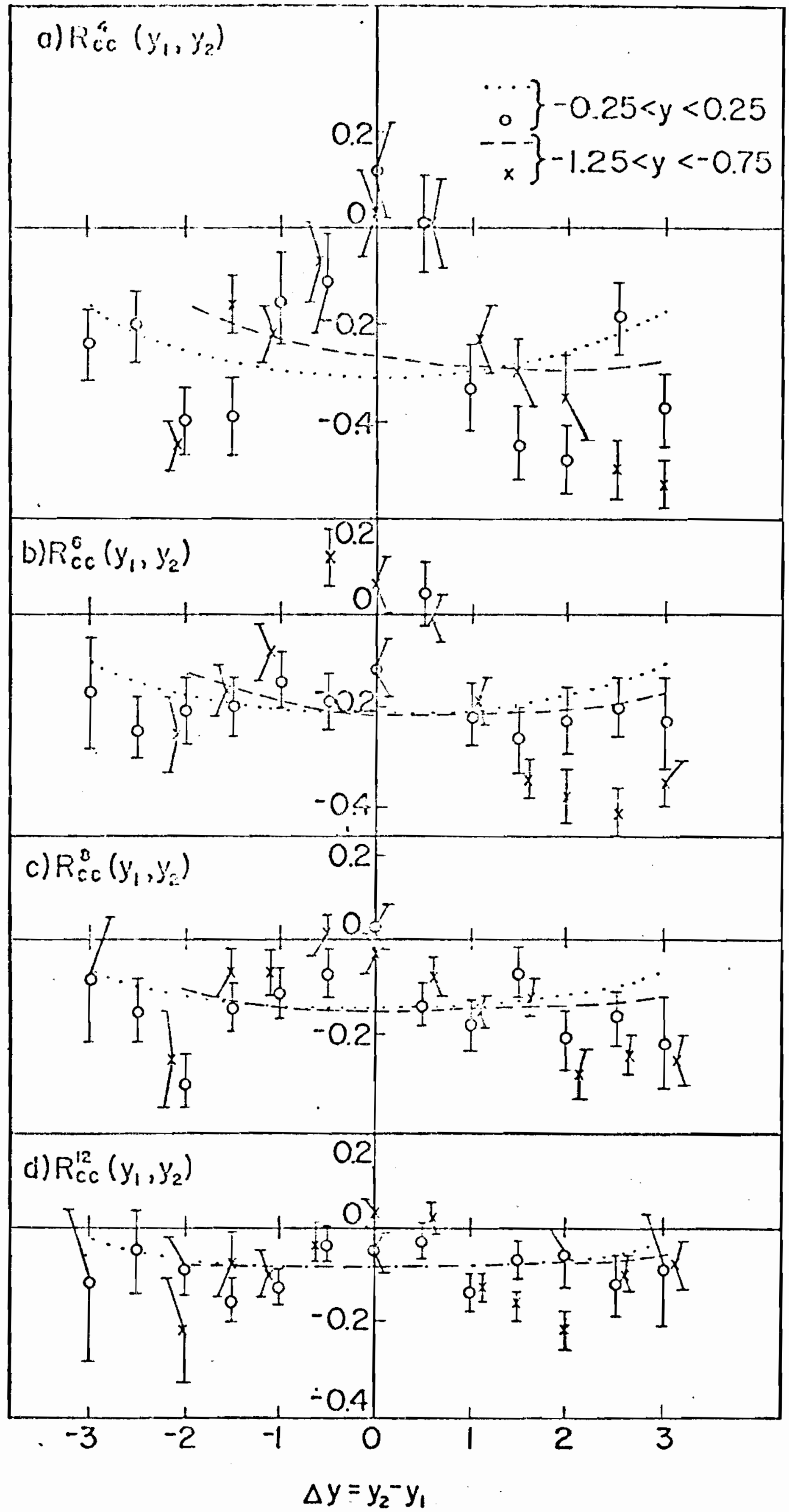

a) $R^4_{cc}(y_1, y_2)$
} −0.25<y <0.25
} −1.25<y <−0.75
b) $R^6_{cc}(y_1, y_2)$
c) $R^8_{cc}(y_1, y_2)$
d) $R^{12}_{cc}(y_1, y_2)$
0.2
0
−0.2
−0.4
−3 −2 −1 0 1 2 3
$\Delta y = y_2 - y_1$

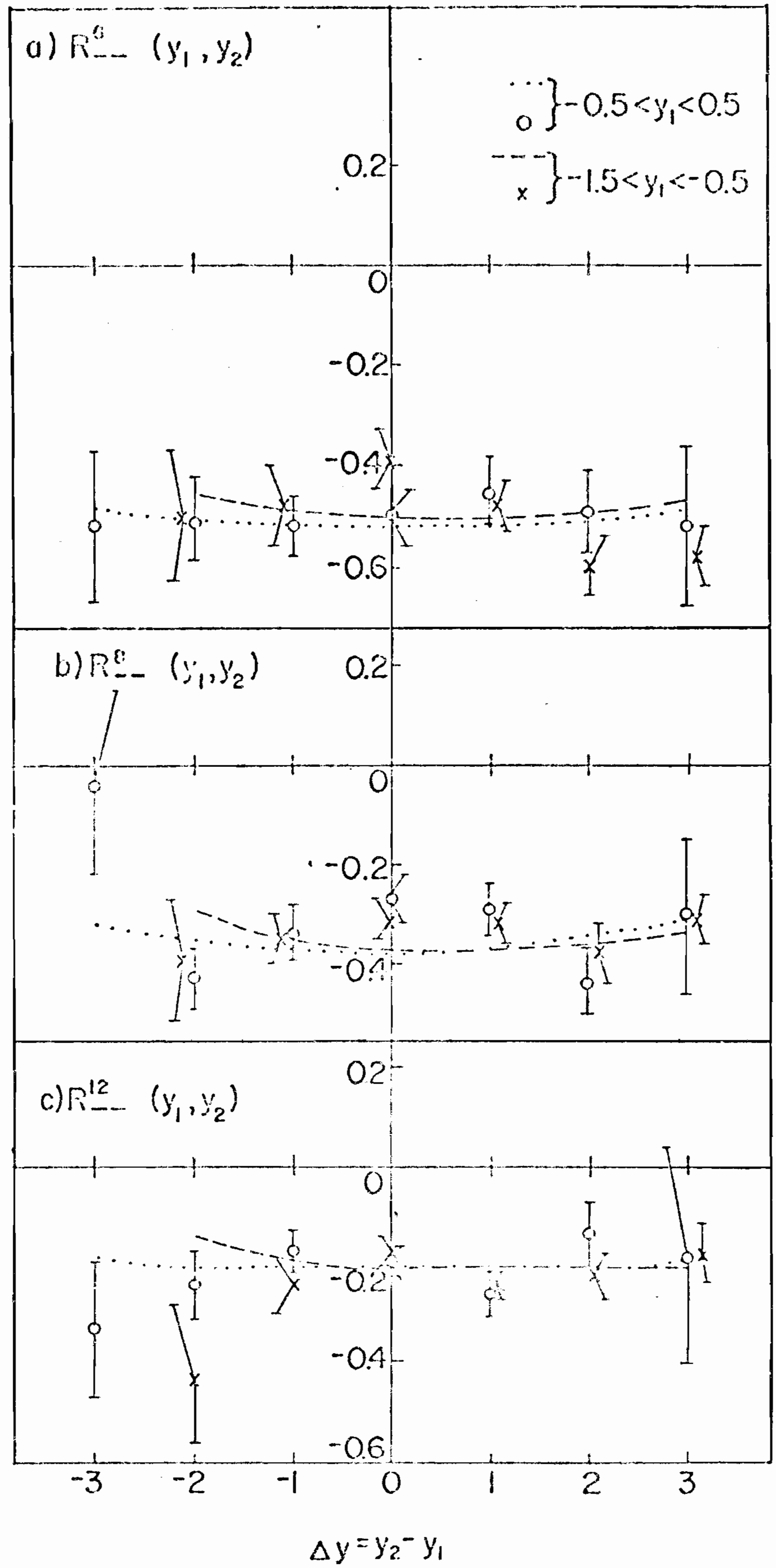

a) R^{8}_{--} (y_1, y_2)
$-0.5<y_1<0.5$
$-1.5<y_1<-0.5$
b) R^{8}_{--} (y_1, y_2)
c) R^{12}_{--} (y_1, y_2)
0.2
0
-0.2
-0.4
-0.6
-3
-2
-1
0
1
2
3
$\Delta y = y_2 - y_1$

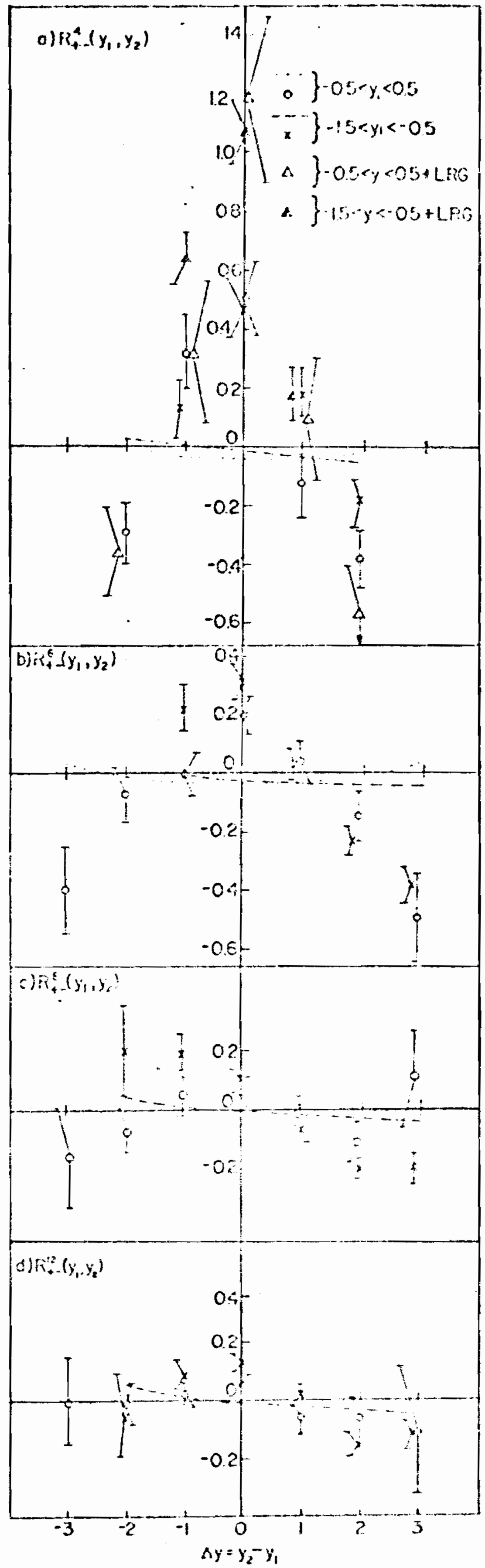

a) $R^4_{+-}(y_1, y_2)$
}-0.5<y₁<0.5
}-1.5<y₁<-0.5
}-0.5<y<0.5+LRG
}-1.5<y<-0.5+LRG
b) $R^6_{+-}(y_1, y_2)$
c) $R^8_{+-}(y_1, y_2)$
d) $R^{12}_{+-}(y_1, y_2)$
$\Delta y = y_2 - y_1$